JOURNAL OF PHYSICAL ORGANIC CHEMISTRY
J. Phys. Org. Chem. 2007; **20:** 610–623
Published online 31 May 2007 in Wiley InterScience
(www.interscience.wiley.com) DOI: 10.1002/poc.1217

Acid assisted proton transfer in 4-[(4-*R*-phenylimino)methyl]pyridin-3-ols: NMR spectroscopy in solution and solid state, X-ray and UV studies and DFT calculations

Almudena Perona,[1]* Dionisia Sanz,[1]* Rosa M. Claramunt,[1] Elena Pinilla,[2] M. Rosario Torres[2] and José Elguero[3]

[1]Departamento de Química Orgánica y Bio-Orgánica, Facultad de Ciencias, UNED, Senda del Rey 9, E-28040 Madrid, Spain
[2]Departamento de Química Inorgánica, Laboratorio de Difracción de Rayos-X, Facultad de Ciencias Químicas, UCM, E-28040 Madrid, Spain
[3]Instituto de Química Médica, CSIC, Juan de la Cierva, 3, E-28006 Madrid, Spain

Received 5 March 2007; accepted 18 April 2007

ABSTRACT: The behaviour of Schiff bases of 3-hydroxy-4-pyridincarboxaldehyde and 4-*R*-anilines (R=H, CH_3, OCH_3, Br, Cl, NO_2) in acid media has been described. ^{1}H, ^{13}C, ^{15}N-NMR chemical shifts allow to establish the protonation site and its influence on the hydroxyimino/oxoenamino tautomerism. DFT calculations, electronic spectra and X-ray diffraction are in agreement with the NMR conclusions. Copyright © 2007 John Wiley & Sons, Ltd.

KEYWORDS: Schiff bases; acid media; tautomerism; hydrogen bonds; NMR spectroscopy; density functional calculations; X-ray; electronic spectra

INTRODUCTION

Transfer of a proton is the basic step in numerous chemical reactions and in many enzymatic processes it becomes the rate-determining step.[1] Double proton transfer among DNA bases has been proposed as a mechanism for DNA mutation.[2] The importance of such phenomenon in biochemical processes has lead to the study of many tautomeric equilibria.

Aromatic Schiff bases of *o*-hydroxyaldehydes are an interesting kind of molecules because of their tautomeric properties related to proton transfer;[3] in general the hydroxyimino tautomer is the only observed form.[4–6] However, the tautomeric equilibrium depends on the solvent,[7] temperature,[8] substituents pattern,[8,9] physical state of the compound[8] and added hosts (i.e. cyclodextrins).[10]

One of the most important Schiff base is the cofactor of the vitamin B_6, pyridoxal-5′-phosphate PLP, involved in the transformation of aminoacids. In the first step of the catalytic cycle the proton transfer occurs in the intramolecular O—H···N hydrogen bond, assisted by protonation of the pyridine ring.[11]

**Correspondence to:* A. Perona, D. Sanz, Departamento de Química Orgánica y Bio-Orgánica, Facultad de Ciencias, UNED, Senda del Rey 9, E-28040 Madrid, Spain.
E-mail: aperona@bec.uned.es; dsanz@ccia.uned.es

The present paper analyses the proton transfer due to the effect of substituents and to the presence of acids on the 3-hydroxypyridine-4-carboxaldehyde aromatic Schiff bases (**8**–**13**) depicted in Scheme 1. ^{1}H, ^{13}C and ^{15}N-NMR spectroscopy have proved to be the best technique to evaluate the tautomeric equilibrium. The conclusions based on NMR studies (both in solution and in the solid state) are supported by computational calculations and UV–Visible studies as well as by one X-ray structure determination.

In previous publications we demonstrated the existence of the intramolecular hydrogen bonded structure present in 4-[(4-*R*-phenylimino)methyl]pyridin-3-ols (R=H, CH_3, OCH_3, Br, Cl, NO_2) (**8**–**13**), prepared from 3-hydroxypyridine-4-carboxaldehyde (**1**) and an equimolar amount of the corresponding 4-*R*-anilines, and confirmed that these compounds exist as hydroxyimino tautomers with (*E*)-configuration.[6]

RESULTS AND DISCUSSION

NMR spectroscopy

In order to study the protonation site and how this affects the acid-base characteristics of the hydrogen bond,

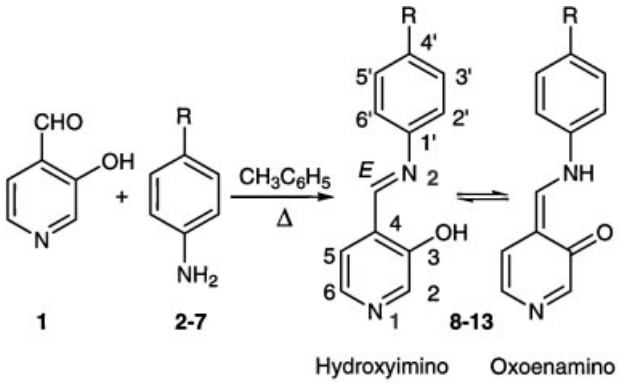

R	H	CH_3	OCH_3	Br	Cl	NO_2
Compound	2	3	4	5	6	7
	8	9	10	11	12	13

Scheme 1. 4-[(4-*R*-Phenylimino)-methyl]-pyridin-3-ol (**8–13**), hydroxyimino/oxoenamino forms

10–20 mg of each imine (**8–13**) were dissolved in trifluoroacetic acid (TFA, $pK_a = 0.2$) and the NMR spectra recorded. In all cases, protonation takes place on the pyridine nitrogen, making these molecules highly sensitive to hydrolysis with partial decomposition into their precursors (Scheme 2). The less stable imines in acid media are those bearing electron-withdrawing substituents and Table 1 shows the relative percentages of compounds in TFA solution after time evolution.

In acid media, the ^{1}H, ^{13}C and ^{15}N-NMR data support the coexistence of both hydroxyimino and oxoenamino tautomers in compounds **8–13**, as we will discuss later on.

The ^{1}H-NMR chemical shifts of compounds **8–13** in neutral and acid media are shown in Table 2. The chemical shift protonation effects on protons H2, H5 and CH=N of the pyridine moiety are significant in imines **8–12**, the most important of ~0.95 ppm for H5 and ~0.65 ppm for CH=N. Moreover, the $J_{5,6}$ coupling constant increases 1 Hz due to protonation.[12] In compound **13**, all protons are only slightly affected save the CH=N that is shifted downfield 0.35 ppm and the H5 shifted downfield 0.77 ppm. Finally, the chemical shifts values of the phenyl group protons close to the tautomeric imine centre, H2′/H6′, increase in all cases on protonation (Fig. 1).

The ^{13}C-NMR chemical shifts of compounds **8–13** in neutral and acid media are gathered in Tables 3 and 4. The assignments of all signals in $CDCl_3$ and TFA at 300 K are based on gs-HMQC and gs-HMBC experiments and the coupling constants values. We already reported that the hydroxyimino and oxoenamino forms can be distinguished by ^{13}C-NMR, the most affected carbon atom when the tautomeric equilibrium changes is that bonded to the oxygen, the corresponding chemical shifts values for other carbons do not significantly vary when the tautomeric form changes.[13] The results found for Schiff bases **8–13** in acid media are very similar: C6 and C1′ chemical shifts decrease around 12 ppm, C2 diminishes about 6 ppm and C5 increases in 6 ppm. These changes can be explained as the result of the

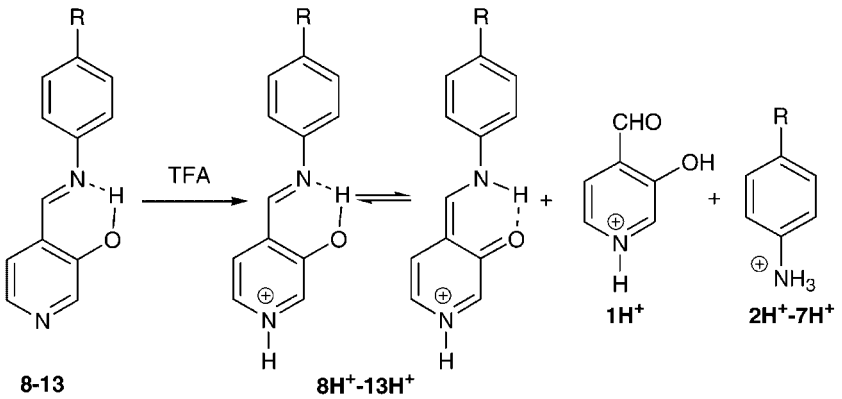

Scheme 2. 4-[(4-*R*-Phenylimino)methyl]pyridinium-3-ols trifluoroacetates (**8H$^+$–13H$^+$**)

Table 1. Relative percentages in TFA solution

	Comp.	H	CH_3	OCH_3	Br	Cl	NO_2
Freshly prepared solution	Imine	75	72	80	58	52	43
	Aldehyde	12.5	14	10	21	24	28.5
	Amine	12.5	14	10	21	24	28.5
5 days	Imine	46	50	44	48	47	33.3
	Aldehyde	27	25	28	26	26.5	33.3
	Amine	27	25	28	26	26.5	33.3

DOI: 10.1002/poc

Table 2. ^{1}H-NMR chemical shifts (δ in ppm) and coupling constants (J in Hz) of **8–13** in neutral and acid media

Comp.	Solvent	CH=N	H2	OH	H5	H6	H2'/H6'	H3'/H5'	R4'
8	$CDCl_3$	8.65(s)	8.52(s)	12.76(sbr)	7.28(d)	8.27(d) $J_{5,6}=4.8$	7.33(m)	7.46(m)	7.35(m)
8H$^+$	TFA	9.30(s)	8.75(s)	—	8.17[a]	8.10[a] $J_{5,6}=6.0$	7.61(m)	7.51(m)	7.51(m)
	$\Delta\delta$	0.65	0.23		0.89	−0.17	0.28	0.05	0.16
9	$CDCl_3$	8.64(sbr)	8.50(sbr)	12.90(sbr)	7.25(m)	8.25(dbr) $J_{5,6}=4.6$	7.25(m)	7.25(m)	2.40(s)
9H$^+$	TFA	9.29(s)	8.82(sbr)	—	8.21[a]	8.17[a] $J_{5,6}=5.7$	7.56(m)	7.35(m)	2.35(s)
	$\Delta\delta$	0.65	0.32		0.96	−0.08	0.31	0.10	−0.05
10	$CDCl_3$	8.55(s)	8.42(s)	12.87(s)	7.17(d)	8.17(d) $J_{5,6}=4.8$	7.26(m)	6.90(m)	3.78(s)
10H$^+$	TFA	9.18(s)	8.84(s)	—	8.21[a]	8.20[a] $J_{5,6}=6.1$	7.70(m)	7.08(m)	3.86
	$\Delta\delta$	0.63	0.42		1.04	0.03	0.44	0.18	0.08
11	$CDCl_3$	8.63(s)	8.52(s)	12.50(sbr)	7.28(d)	8.28(d) $J_{5,6}=4.9$	7.20(m)	7.59(m)	—
11H$^+$	TFA	9.25(s)	8.71(s)	—	8.13[a]	8.11[a] $J_{5,6}=6.0$	7.65(m)	7.48(m)	—
	$\Delta\delta$	0.66	0.23		0.89	−0.13	0.45	−0.11	
12	$CDCl_3$	8.60(s)	8.50(s)	12.50(sbr)	7.24(d)	8.26(d) $J_{5,6}=4.9$	7.25(m)	7.41(m)	—
12H$^+$	TFA	9.24(s)	8.71(s)	—	8.14[a]	8.12[a] $J_{5,6}=6.0$	7.58(m)	7.48(m)	—
	$\Delta\delta$	0.64	0.21		0.90	−0.12	0.33	0.07	
13	$CDCl_3$	8.67(s)	8.57(s)	12.06(sbr)	7.34(d)	8.33(d) $J_{5,6}=5.0$	7.37(m)	8.35(m)	—
13H$^+$	TFA	9.02(s)	8.51(s)	—	8.11(d)	8.26(d) $J_{5,6}=5.9$	7.57(m)	8.33(m)	—
	$\Delta\delta$	0.35	−0.06		0.77	−0.07	0.20	−0.02	

[a] These protons show an AB system, the assignments are based on gs-HMQC experiments and on the coupling constant values $^1J_{C5H5} < {}^1J_{C6H6}$.

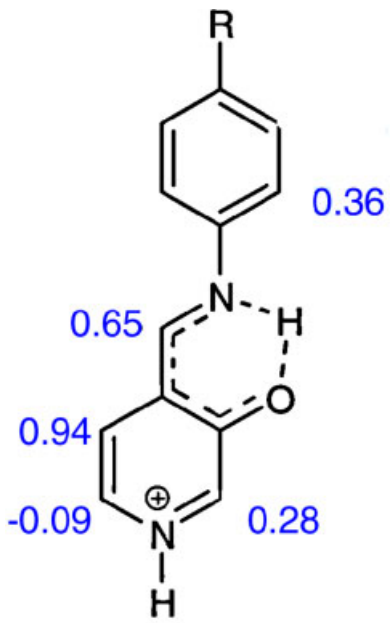

Figure 1. Protonation effects in the ^{1}H-NMR chemical shifts [$\Delta\delta$(TFA-$CDCl_3$)] of compounds **8–12**. This figure is available in colour online at www.interscience.wiley.com/journal/poc

pyridine nitrogen protonation that leads in solution to the coexistence of the two tautomeric protonated forms in equilibrium. The phenyl moiety, due to intrinsic *R* substituent effects, is not useful for equilibrium studies (Fig. 2).

Similarly, Table 5 reports the ^{15}N chemical shifts of N1 and N2 for compounds **8–13** in neutral and acid media, the assignments are based on gs-HMBC spectra (Fig. 3). In the case of N1, the $\Delta\delta$ values (−120 to −130 ppm) are characteristic of pyridine protonation.[14] The values of N2 obtained in TFA for **8–12** are intermediate between the typical chemical shifts of hydroxyimino (approximately −55.5 ppm) and oxoenamino (approximately −285 ppm) nitrogen atoms,[8,13–15] pointing out to a rapid proton exchange between the two tautomers (Fig. 4). On the other hand, the chemical shifts of N2 of 4-(4-nitrophenylimino)methyl]pyridin-3-ol (**13**) in neutral and acid media are very close ($\Delta\delta = -0.8$ ppm), indicating that the hydroxyimino form is the predominant one in both media (>99%) for such derivative. The reason for such behaviour can be explained as due to the *p*-nitro group effect that diminishes the electron density on the imino nitrogen.

DOI: 10.1002/poc

Table 3. ^{13}C-NMR chemical shifts (δ in ppm) and coupling constants (J in Hz) for the pyridine moiety of **8–13**

Comp.	Solvent	CH=N	C2	C3	C4	C5	C6
8	$CDCl_3$	160.9	141.2	155.1	123.6	123.6	140.3
		$^1J=163.6$	$^1J=180.8$			$^1J=161.0$	$^1J=179.9$
		$^3J=6.2$	$^3J=10.3$			$^3J=9.2$	$^3J=11.0$
8H$^+$	TFA	158.3	135.0	162.3	125.7	130.6	127.9
		$^1J=183.5$	$^1J=193.3$			$^1J=174.6$	$^1J=198.0$
		$^3J=6.1$	$^3J=5.9$				$^3J=5.0$
	$\Delta\delta$	−2.6	−6.2	7.2	2.1	7.0	−12.4
9	$CDCl_3$	159.6	140.9	155.1	123.6	123.4	140.2
		$^1J=163.4$	$^1J=180.8$	$^3J=^3J=^2J=7.3$		$^1J=161.0$	$^1J=181.5$
		$^3J=6.3$	$^3J=11.1$			$^3J=9.2$	$^3J=11.4$
9H$^+$	TFA	156.2	134.6(br)	157.5	126.3(br)	130.5	128.6
		$^1J=184.4$	$^1J=191.6$	$^2J=3.1$		$^1J=175.9$	$^1J=194.7$
		$^3J=6.1$		$^3J=8.0$			
	$\Delta\delta$	−3.4	−6.3	2.4	2.7	7.1	−11.6
10	$CDCl_3$	158.2	141.1	155.1	123.8	123.4	140.4
		$^1J=163.1$	$^1J=181.0$			$^1J=160.7$	$^1J=182.3$
		$^3J=6.2$	$^3J=^3J=9.3$			$^3J=9.0$	$^3J=11.9$
10H$^+$	TFA	153.1	133.9	160.8	126.8	130.0	129.2
		$^1J=185.8$	$^1J=193.4$			$^1J=174.8$	$^1J=198.2$
	$\Delta\delta$	−5.1	−7.2	5.7	3.0	6.6	−11.2
11	$CDCl_3$	161.3	141.2	154.9	123.3	123.6	140.4
		$^1J=163.6$	$^1J=181.8$			$^1J=161.0$	$^1J=182.0$
		$^3J=6.2$	$^3J=10.3$			$^3J=10.1$	$^3J=10.7$
11H$^+$	TFA	158.2	134.7	162.4	127.2	129.9	127.8
		$^1J=181.5$	$^1J=195.0$			$^1J=173.8$	$^1J=195.1$
		$^3J=5.3$					
	$\Delta\delta$	−3.1	−6.5	7.5	3.9	6.3	−12.6
12	$CDCl_3$	161.1	141.0	154.8	123.2	123.5	140.3
		$^1J=163.7$	$^1J=181.1$			$^1J=161.1$	$^1J=182.6$
		$^3J=6.2$	$^3J=10.7$			$^3J=9.1$	$^3J=12.5$
			$^3J=5.8$				
12H$^+$	TFA	158.2	134.7	162.4	126.9	129.9	127.8
		$^1J=180.9$	$^1J=192.0$			$^1J=173.9$	$^1J=196.4$
	$\Delta\delta$	−2.9	−6.3	7.6	3.9	6.4	−12.5
13	CD_3CN	166.8	141.8	155.9	124.6	125.8	141.7
		$^1J=168.2$	$^1J=181.7$	$^3J=^3J=4.9$		$^1J=163.6$	$^1J=182.0$
		$^3J=5.9$	$^3J=10.2$			$^3J=9.9$	$^3J=10.1$
13H$^+$	TFA	161.2	132.7	159.5	130.2	128.7	130.0
		$^1J=174.8$	$^1J=191.8$	$^3J=6.1$		$^1J=175.6$	$^1J=197.0$
		$^3J=6.0$					
	$\Delta\delta$	−5.6	−9.1	3.6	5.6	2.9	−11.7

To verify that TFA, which modifies the acidity of the media and the polarity around the hydrogen bonds, stabilizes the oxoenamino *versus* the hydroxyimino tautomer, we decided to prepare the tetrafluoroborate salts **10H$^+$BF$_4^-$**, **11H$^+$BF$_4^-$** plus the complex **11·Picric acid** to study them in solid state comparatively to solution by NMR spectroscopy. The CPMAS NMR spectroscopy has been already used to elucidate Schiff bases structure.[15–17] In the solid state, where the signals are not averaged by solvent effects or by rapid exchange processes often present in solution, the change in the nitrogen chemical shifts caused by complete protonation can be of the order of 50–100 ppm, allowing a more accurate study.[18–20]

From the ^{1}H-NMR data, these salts exist in the hydroxyimino form. In THF-d_8 two different salt species are observed and no evolution with time was observed. Similarly occurs in DMSO-d_6 solution, the minor species evolving towards the major one after 12 h; the OH chemical shift was detected only in DMSO-d_6 as a very broad signal at 9.70 ppm. In CD_3OD addition of the solvent to the double imino bond occurs, the imino proton shifts upfield from 9.12 to 5.90 ppm (Experimental Part).

The ^{13}C-NMR data for salts **10H$^+$BF$_4^-$**, **11H$^+$BF$_4^-$** and **11·Picric acid** are shown in Table 6 (gs-HMQC and gs-HMBC spectra were used for the assignments). For tetrafluoroborate salts **10H$^+$BF$_4^-$**, **11H$^+$BF$_4^-$** no significant differences between neutral imines and their salts appear, and the signals used to be very broad in solid state (e.g. in Fig. 5). The ^{15}N-NMR chemical shifts show that the pyridine nitrogen is protonated and only the hydroxyimino form is present (Table 7, Fig. 6). In

DOI: 10.1002/poc

Table 4. ^{13}C-NMR chemical shifts (δ in ppm) and coupling constants (J in Hz) for the phenyl moiety of **8–13**

Comp.	Solvent	C1′	C2′	C3′	C4′	*R*
8	$CDCl_3$	147.6 $^3J=^3J=^3J=8.7$	121.2 $^1J=160.4$ $^3J=6.2$ $^4J=5.5$	129.5 $^1J=161.8$ $^3J=8.0$	128.0 $^1J=163.0$ $^3J=^3J=7.6$	—
8H$^+$	TFA	134.7	120.4 $^1J=164.1$ $^3J=^3J=6.0$	129.9 $^1J=167.0$ $^3J=7.7$	132.9 $^1J=165.3$ $^3J=^3J=7.1$	
	$\Delta\delta$	−12.9	−0.8	0.4	4.9	
9	$CDCl_3$	144.8 $^3J=^3J=^3J=7.3$	121.1 $^1J=159.6$ $^3J=4.1$	130.1 $^1J=158.3$ $^3J_{(CH_3)}=5.0$ $^3J=5.0$	138.3 $^3J_{(H2\prime/H6\prime)}=^2J_{(CH_3)}=6.3$	21.0 $^1J=126.6$ $^3J=^3J=3.6$
9H$^+$	TFA	131.9	120.4 $^1J=162.0$	130.7 $^1J=161.3$ $^3J=4.6$	140.8 $^3J_{(H2\prime/H6\prime)}=^2J_{(CH_3)}=6.3$	19.0 $^1J=127.8$ $^3J=4.0$
	$\Delta\delta$	−12.9	−0.7	0.6	2.5	−2
10	$CDCl_3$	140.36	122.7 $^1J=159.3$ $^3J=6.2$	114.8 $^1J=160.3$ $^3J=5.2$	159.8	55.6 $^1J=144.1$
10H$^+$	TFA					
	127.8	122.9 $^1J=163.5$ $^3J=5.5$	115.6 $^1J=165.6$ $^3J=4.7$	164.0	54.5 $^1J=146.2$	
	$\Delta\delta$	−12.6	0.2	0.8	4.2	−1.2
11	$CDCl_3$	146.5 $^3J=^3J=^3J=8.3$	122.8 $^1J=161.6$ $^3J=5.8$	132.6 $^1J=167.2$ $^3J=6.0$	121.7 $^3J=^3J=9.8$	—
11H$^+$	TFA	135.5	121.8 $^1J=165.9$ $^3J=5.0$	133.2 $^1J=172.1$ $^3J=5.5$	127.0	—
	$\Delta\delta$	−11	−1	0.6	5.3	
12	$CDCl_3$	145.8 $^3J=^3J=^3J=8.8$	122.4 $^1J=163.2$ $^3J=5.8$	129.5 $^1J=167.6$ $^3J=5.4$	133.6 $^3J=^3J=10.1$ $^2J=^2J=3.2$	—
12H$^+$	TFA	135.0	121.7 $^1J=165.3$ $^3J=5.5$	130.1 $^1J=170.9$ $^3J=5.2$	139.4	—
	$\Delta\delta$	−10.8	−0.7	0.6	5.8	
13	CD_3CN	154.5 $^3J=8.1$	123.6 $^1J=166.4$ $^3J=5.7$	126.2 $^1J=169.9$ $^3J=4.6$	147.8	—
13H$^+$	TFA	147.0	121.7 $^1J=167.1$ $^3J=5.6$	124.7 $^1J=171.5$ $^3J=5.1$	149.2	—
	$\Delta\delta$	−7.5	−1.9	−1.5	1.4	

11·Picric acid the acidity of picric acid (2,4,6-trinitrophenol, $pK_a=0.4$) is not strong enough to protonate the pyridine nitrogen, as we can observe in the N1 chemical shift of Table 7; possibly this nitrogen atom is coordinated through hydrogen bonding to the OH of the picric acid, thus the compound is not a picrate but a picric acid complex.[21] The ^{13}C chemical shift values of the picric acid, C1″, C2″ and C4″ in the Experimental Part, also indicate that the hydroxyl proton is transferred in some amount towards the pyridine nitrogen. The presence of different signals for N1 and N2 in the ^{15}N CPMAS NMR spectrum of **11H**$^+$**BF**$_4^-$ suggests the existence either of different conformations or polymorphs.

X-Ray crystallographic studies

The molecular structure of a compound being dependent on its physical state, different tautomeric forms can be found in solution, in the crystal and in the gas phase.[22] Concerning the present work, X-ray diffraction studies

DOI: 10.1002/poc

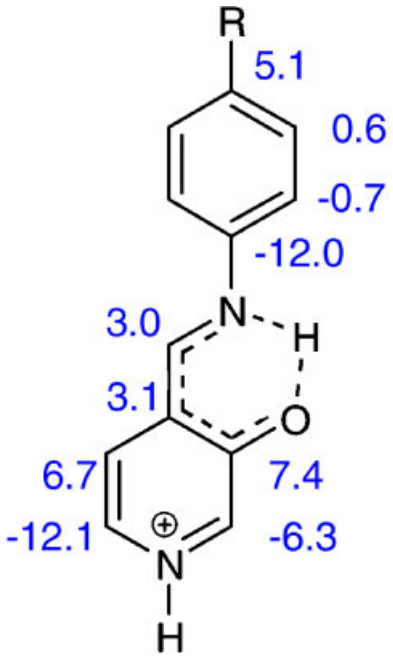

Figure 2. Protonation effects in the ^{13}C-NMR chemical shifts [$\Delta\delta$(TFA-$CDCl_3$)] of compounds **8–13**. This figure is available in colour online at www.interscience.wiley.com/journal/poc

show that (*E*)-4-[(4-bromophenylimino)methyl]-3-hydroxypyridinium tetrafluoroborate (**11H$^+$BF$_4^-$**) exists exclusively in the hydroxyimino form in the crystal at room temperature, in agreement with the CPMAS NMR data. Attempts to get good quality crystals of **10H$^+$BF$_4^-$** and **11·Picric acid** for X-ray diffraction analysis proved to be unsuccessful.

The structure of the cation **11H$^+$** showing the atomic numbering is shown in Fig. 7 and selected distances and angles are listed in Table 8. The driving force for the observed planarity is the intramolecular hydrogen bond N2···H1B-O1, which locks the imine group into the planar configuration even in the presence of the water molecule,[23] where O2A binds the pyridine nitrogen through H1A-N1. The hydrogen atoms of the water molecule were not observed in the difference maps and are not shown, but O···Br [mean value of 3.65(2) Å] and O···F [in the range 2.63(3)–2.91(3) Å] distances are consistent with hydrogen-bonding formation between the heteroatoms.

The N1-H1A···O2A and Br··O hydrogen bonds lead to the formation of dimers in the packing, which also present π–π stacking interactions between the phenyl and pyridinium rings. The distance between the ring centroids is 3.79 Å and the angle between the ring normal and the vector between the ring centroids is of 21.23, since one ring is slipped 1.38 Å relative to the opposite molecule.[24] Additionally the O···F(BF_4) hydrogen bonds give rise to undulated layers parallel to (100) as depicted in Fig. 8.

Table 5. ^{15}N-NMR chemical shifts (δ in ppm) of **8–13**

Compound	Solvent	N1	N2
8	$CDCl_3$	−56.6	−67.5
8H$^+$	TFA	−178.1	−166.4
	$\Delta\delta$	−121.5	−98.9
9	$CDCl_3$	−57.7	−69.1
9H$^+$	TFA	−176.0	−167.7
	$\Delta\delta$	−118.3	−98.6
10	$CDCl_3$	−57.5	−70.5
10H$^+$	TFA	−178.1	−168.7
	$\Delta\delta$	−120.6	−98.2
11	$CDCl_3$	−55.0	−71.4
11H$^+$	TFA	−179.6	−149.2
	$\Delta\delta$	−124.6	−77.8
12	$CDCl_3$	−55.8	−70.6
12H$^+$	TFA	−179.6	−149.2
	$\Delta\delta$	−123.8	−78.6
13	CD_3CN	−50.5	−75.5
13H$^+$	TFA	−181.2	−76.3
	$\Delta\delta$	−131.2	−0.8

Theoretical calculations

The hybrid DFT B3LYP/6-31G** method[25,26] was used to carry out the optimisation of the structures and no restrictions were imposed, save the initial angle C4CHN that was set to 0° in order to form the intramolecular —OH···N=C< hydrogen bond. After each geometry optimisation, the vibrational frequencies were computed in order to ensure that the calculated geometry corresponds to a minimum and not to a saddle point on the energy hypersurface.

At the same theoretical level we had already established that in neutral imines the hydroxyimino tautomer with *E* configuration is the most stable.[6] Taking this structure as the starting point, the Schiff bases **8–13** present three different positions to be protonated by TFA (N1, N2 and OH). The results on the geometry optimisation of the different structures point out that protonation are clearly favoured at the pyridine nitrogen (N1) over protonation at the other sites. According to calculations, in the gas phase, the protonated oxoenamino form is only 3–7 kJ mol^{-1} higher in energy than the protonated hydroxyimino one (Table 9). Therefore, theoretical results would predict that in solution or in solid state the two protonated forms can be present.

In hydrogen bonds the heavy atoms are separated by less than the sum of their van der Waals radii, that is, for weak HBs, N···H···O $\leq$ 2.7 Å, whereas in strong HBs the separation is 2.5–2.6 Å for N···H···O.[27] When the proton moves towards the centre of the hydrogen bond, a contraction of the N···O distance is observed. The HB distances summarised in Table 10 show a shorter value for the protonated form, therefore the hydrogen bond becomes stronger, with the nitrogen atom and the proton closer making the proton transfer easier.

DOI: 10.1002/poc

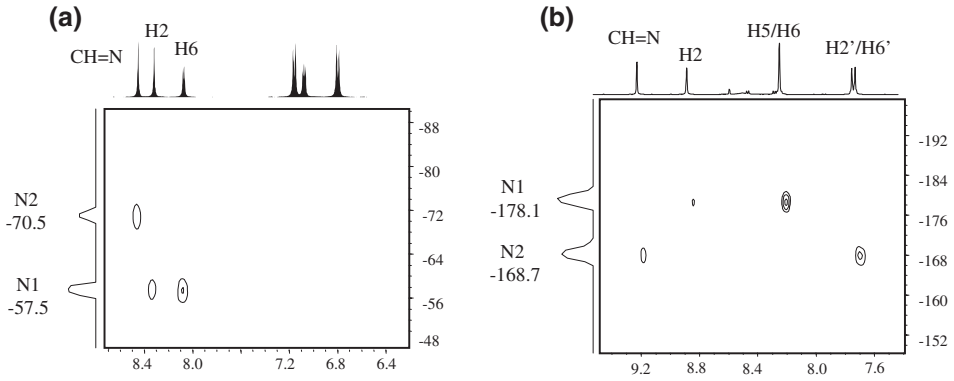

Figure 3. ^{15}N-NMR of **10** in solution: (a) $CDCl_3$, (b) in CF_3COOH

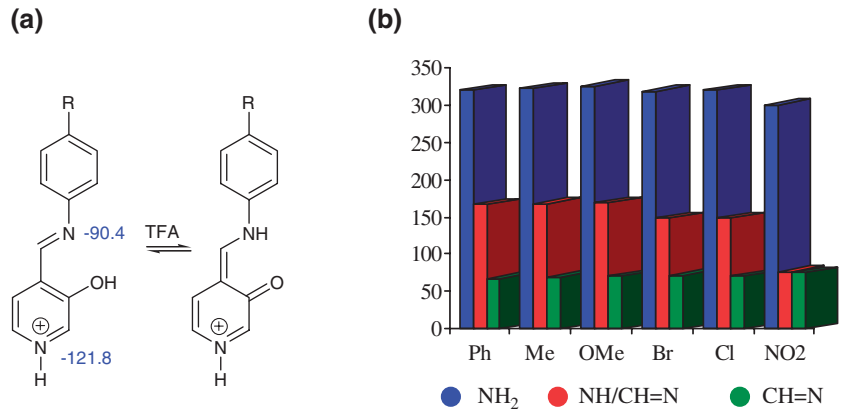

Figure 4. (a) Protonation effects in the ^{15}N-NMR chemical shift [$\Delta\delta$(TFA-$CDCl_3$)] of compounds **8**–**12**, (b) Chemical shift values ($-\delta$ in ppm) of N2 for **8**–**13** oxoenamino/hydroxyimino forms (red), hydroxyimino forms (green) and the anilines **2**–**7** (blue)

Electronic spectra

The wavelength absorption bands (λ_{max} in nm) in the electronic spectra of the Schiff bases **8**–**13** in acetonitrile (absorption at <190 nm) and the corresponding absorption band in 0.1 M TFA in CH_3CN are shown in Table 11. These absorptions mainly represent the pyridine chromophore.[6] Figure 9 shows the electronic spectra in neutral and acid media of 3-hydroxypyridine-4-carboxaldehyde (**1**) and two of the Schiff bases studied, the

Table 6. ^{13}C-NMR chemical shifts (δ in ppm) and coupling constants (J in Hz) for the pyridine moiety of **10H$^+$BF$_4^-$**, **11H$^+$BF$_4^-$** and **11·Picric acid**

Compound	Solvent	CH=N	C2	C3	C4	C5	C6
10H$^+$ BF$_4^-$	DMSO-d_6	155.2	133.2	156.3	132.0	125.9	133.5
		$^1J = 172.3$	$^1J = 188.6$	$^3J = 4.6$		$^1J = 171.7$	$^1J = 191.3$
		$^3J = 5.3$	$^3J = 8.1$	$^3J = 7.1$		$^3J = 6.0$	$^3J = 7.2$
						$^2J = 2.4$	$^2J = 4.2$
	THF-d_8	157.5[a]	133.6	158.8	135.0	128.7	134.1
		157.6[b]	135.0	157.6	134.9	127.8	134.8
	CP-MAS	153.9	132.1	157.6	130.3	130.0	132.1
					127.4		
11H$^+$ BF$_4^-$	THF-d_8	162.8[a]	135.5	158.4	123.7	128.2	135.8
		161.5[b]	135.2	[c]	[c]	128.2	[c]
	CP-MAS	157.7	133.4	158.6	130.0	130.6	133.4
11·Picric acid	DMSO-d_6	158.0	134.7	155.7	124.3	125.2	134.4
		$^1J = 171.6$	$^1J = 186.5$				$^1J = 186.5$

[a] Major product.
[b] Minor product.
[c] Not observed.

DOI: 10.1002/poc

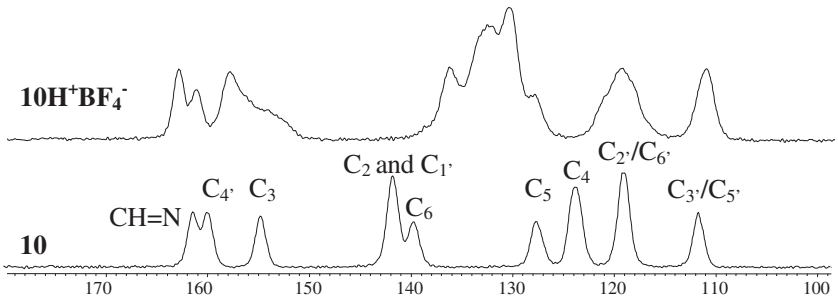

Figure 5. ^{13}C CPMAS NMR of (*E*)-4-[(4-methoxyphenylimino)methyl]-3-hydroxypyridine (**10**) and its tetrafluoroborate salt **10H$^+$BF$_4^-$**

Table 7. ^{15}N-NMR chemical shifts (δ in ppm) of **10H$^+$BF$_4^-$**, **11H$^+$BF$_4^-$** and **11·Picric acid**

Compound	Solvent	N1	N2
10H$^+$ BF$_4^-$	DMSO-d_6	−157.1	−58.7
	THF-d_8	−154.0[a]	−68.0
		−177.3[b]	−66.0
	CP-MAS	−180.0	−70.7
11H$^+$ BF$_4^-$	THF-d_8	[c]	−68.3
	CP-MAS	−177.5	−71.2
		−178.3	−72.1
		−179.9	−72.8
		−181.2	
11·Picric acid[d]	DMSO-d_6	−137.6	−54.8

[a] Major product.
[b] Minor product.
[c] Not observed.
[d] Picric acid ^{15}N-NMR δ (ppm): −12.6 (NO_2), −9.5 (NO_2).

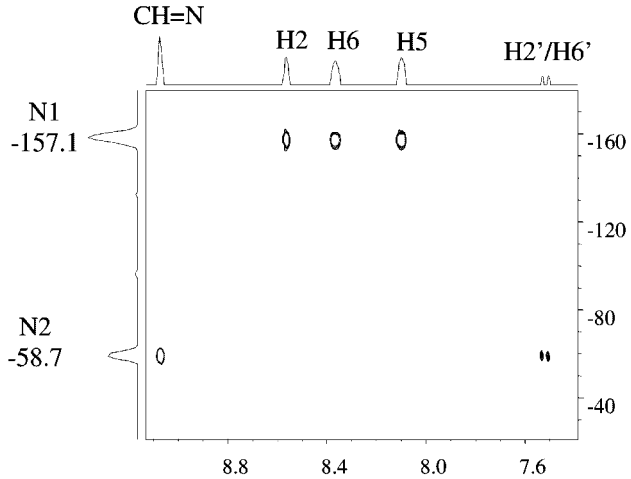

Figure 6. gs-HMBC ^{15}N-NMR of (*E*)-4-[(4-methoxyphenylimino)methyl]-3-hydroxypyridinium tetrafluoroborate (**10H$^+$BF$_4^-$**) in DMSO-d_6

4-[(4-methoxyphenylimino)methyl]pyridin-3-ol (**10**) and the 4-[(4-nitrophenylimino)methyl]pyridin-3-ol (**13**). Comparing the two spectra we notice that in the aldehyde the protonation of the pyridine nitrogen red-shifted the absorption band of the pyridine chromophore (Fig. 9a), but in the Schiff bases the longer wavelength absorption bands are blue-shifted (Fig. 9b) suggesting the presence of the oxoenamino tautomer in equilibrium with the hydroxyimino.[28] To confirm our proposal we recorded the ^1H, ^{13}C and ^{15}N-NMR in 0.5M TFA in CD_3CN of **10**, the chemical shifts indicate the expected equilibrium between the two tautomeric forms: ^1H-NMR δ: 9.06 (s, CH═N), 8.43 (s, H2), 8.13 (d, H6, $^3J = 5.97$ Hz), 8.05 (d, H5), 7.63 (m, H2′/H6′), 7.07 (m, H3′/H5′), 3.84 (s, OCH_3); ^{13}C-NMR δ: 157.9 (CH═N), 134.9 (C2), 131.3 (C5), 130.8 (C6), 126.0 (C4), 125.6 (C2′/C6′), 117.0 (C3′/C5′), 56.9 (OCH_3); ^{15}N-NMR δ: −109.7 (N2), −180.0 (N1). Only in the 4-[(4-nitrophenylimino)methyl] pyridin-3-ol (**13**) such blue-shift was not observed (Fig. 9c), indicating that there was no proton transfer between the

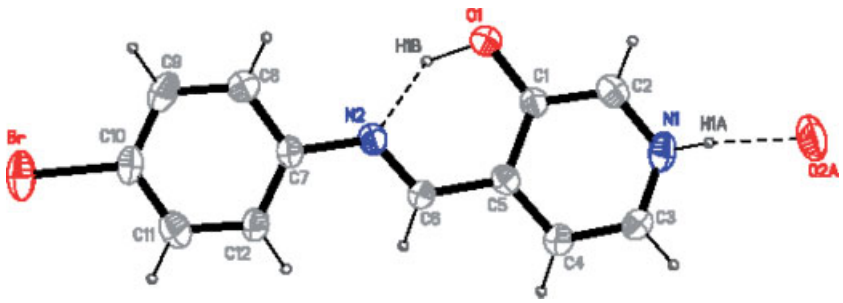

Figure 7. ORTEP plot of (*E*)-4-[(4-bromophenylimino)methyl]-3-hydroxypyridinium tetrafluoroborate (**11H$^+$BF$_4^-$**) with thermal ellipsoids at 30% probability. The BF_4 anion is omitted for clarity purposes

DOI: 10.1002/poc

Table 8. Selected bond lengths [Å] and angles [°] including hydrogen bonds for **11H$^+$BF$_4^-$**

Br-C10	1.884(8)	C11-C10-Br	119.7(7)
N2-C7	1.435(9)	C9-C10-Br	120.3(6)
N2-C6	1.259(9)	C6-N2-C7	122.7(7)
C5-C6	1.46(1)	N2-C6-C5	121.3(7)
C1-O1	1.337(8)	C1-C5-C6	120.3(7)
N1-C2	1.34(1)	O1-C1-C5	121.8(7)
N1-C3	1.31(1)	C2-C1-O1	119.6(7)
O1-H1B	1.1025	C3-N1-C2	122.0(7)
N1-H1A	0.8645	C1-O1-H1B	107.7
O1···N2	2.563(8)	C3-N1-H1A	118.9
N1···O2A[a]	2.68(2)	C2-N1-H1A	117.8
N1···O2B[a]	2.77(2)	O1-H1B···N2	138.0
H1B···N2	1.64	N1-H1A···O2A[a]	170.5
H1A···O2B[a]	1.94	N1-H1A···O2B[a]	162.2
H1A···O2A[a]	1.83		

[a] Oxygen atom of water molecule with 0.5/0.5 occupancy.

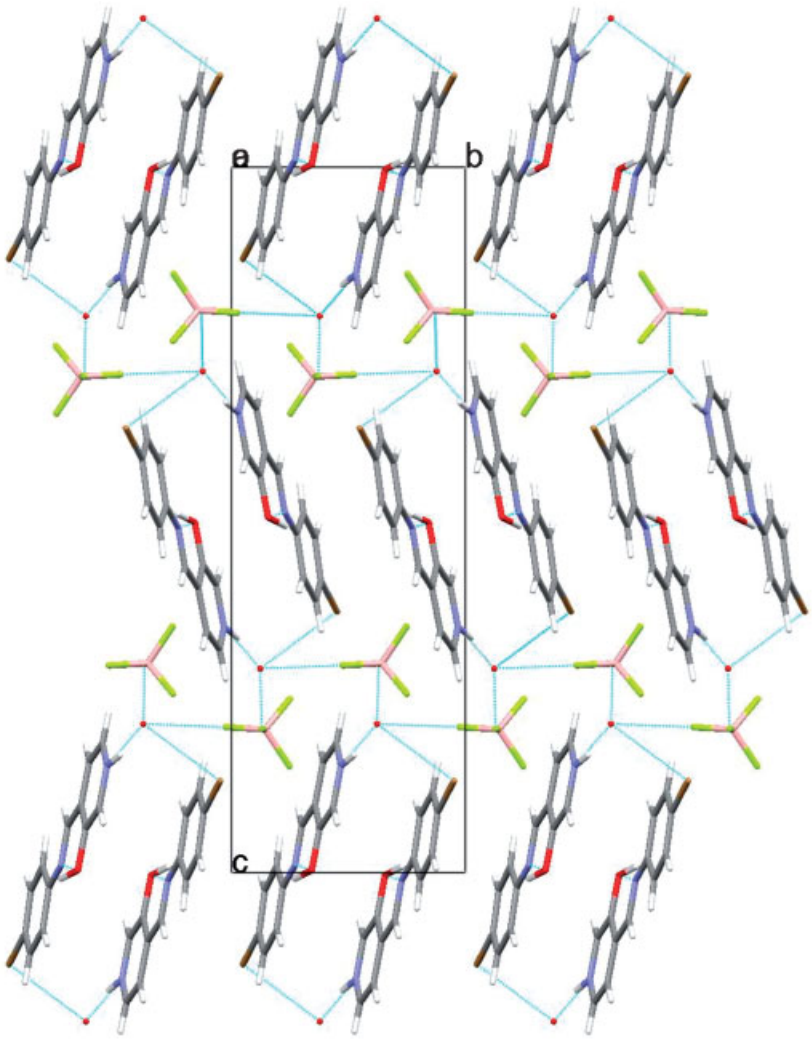

Figure 8. Crystal packing of (*E*)-4-[(4-bromophenylimino)methyl]-3-hydroxypyridinium tetrafluoroborate (**11H$^+$BF$_4^-$**) along **a**. The fluorine atoms and the water oxygen are represented only in one of the two disordered positions

DOI: 10.1002/poc

Table 9. Absolute energies (hartrees) and relative energies (kJ mol^{-1}) of structures **8H$^+$**–**13H$^+$**

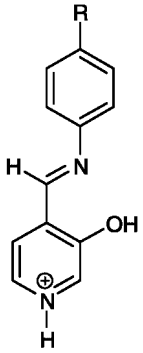

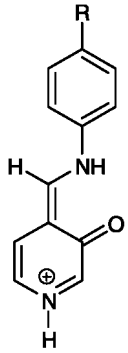

Compound		Hydroxyimino	Oxoenamino
8H$^+$(R═H)		−648.42433 (0.0)	2.99
	+ZPE	−648.21482 (0.0)	4.00
9H$^+$(R═CH_3)		−687.74823 (0.0)	3.52
	+ZPE	−687.51132 (0.0)	3.84
10H$^+$(R═OCH_3)		−762.95747 (0.0)	6.25
	+ZPE	−762.71511 (0.0)	6.67
11H$^+$(R═Br)		−3221.70012 (0.0)	5.38
	+ZPE	−3221.50081 (0.0)	5.93
12H$^+$(R═Cl)		−1108.01520 (0.0)	5.59
	+ZPE	−1107.81540 (0.0)	6.23
13H$^+$(R═NO_2)		−852.91163 (0.0)	5.91
	+ZPE	−852.69953 (0.0)	5.89

imino nitrogen and the OH group and that the oxoenamino form is not present. The overall results agree with those obtained by NMR spectroscopy in TFA. The electronic spectra of the tetrafluoroborate salts of imines **10** and **11** were also registered, the wavelength absorption bands in acetonitrile [λ_{max} in nm, (logε)] being: **10H$^+$BF$_4^-$** 385.0 (4.17), **11H$^+$BF$_4^-$** 359.5 (4.12) and $\Delta\lambda$(**10H$^+$ BF$_4^-$ −10**) = 30 nm, $\Delta\lambda$(**11H$^+$ BF$_4^-$ −11**) = 30 nm.

CONCLUSIONS

A set of novel ^{1}H, ^{13}C and ^{15}N-NMR data of aromatic Schiff bases, 4-[(4-*R*-phenylimino)methyl]pyridin-3-ols (R═H, CH_3, OCH_3, Br, Cl, NO_2), in acid solution has been determined showing that the transfer of the bridging proton of the intramolecular O—H···N hydrogen bond from the hydroxyl oxygen to the imino proton is assisted by protonation of the pyridine ring. A comparison of the solution results with the data obtained for the tetrafluoroborate salts in solid state by CPMAS NMR and X-ray analysis has demonstrated that protonation takes place on the pyridine nitrogen but the compounds still exist in the hydroxyimino form in solid state.

An increase in the solvent acidity changes the polarity around the hydrogen bond and shifts the equilibrium from hydroxyimino towards oxoenamino tautomers. The magnitude of the effect is related to the solvent capacity to protonate the pyridine ring.[29]

Table 10. Hydrogen bond distances r_{N_2H}/r_{N_2O}

Compound	Hydroxyimino	HydroxyiminoH$^+$	Δr
8	1.747 Å/2.638 Å	1.653 Å/2.572 Å	0.094/0.066
9	1.745 Å/2.637 Å	1.653 Å/2.572 Å	0.092/0.065
10	1.744 Å/2.638 Å	1.656 Å/2.575 Å	0.088/0.063
11	1.755 Å/2.643 Å	1.659 Å/2.575 Å	0.096/0.068
12	1.754 Å/2.642 Å	1.661 Å /2.576 Å	0.093/0.066
13	1.766 Å/2.649 Å	1.677 Å /2.584 Å	0.089/0.065

DOI: 10.1002/poc

Table 11. The wavelength absorption bands in the electronic spectra of **1**, **8**–**13**, λ_{max} in nm, (logε)

Compound	CH_3CN	0.1 M TFA in CH_3CN	$\triangle\lambda$
1	332.5 (3.63)	320.5 (3.79)	−12
8	338.5 (3.94)	354.0 (4.05)	15.5
9	342.5 (4.10)	365.5 (4.21)	23
10	355.0 (4.19)	394.0 (4.27)	39
11	328.5 (4.07)	361.0 (4.20)	32.5
12	329.5 (4.03)	360.5 (4.14)	31
13	329.0 (3.96)	322.0 (4.04)	−7

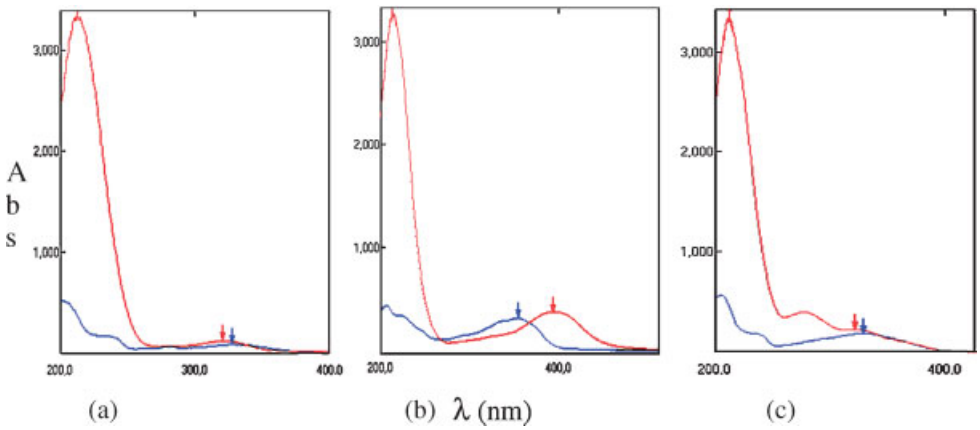

Figure 9. Electronic spectra in CH_3CN (blue) and 0.1M TFA in CH_3CN (red) of compounds: (a) **1**, (b) **10**, (c) **13**

EXPERIMENTAL PART

General procedures

Melting points were determined by DSC on a SEIKO DSC 220C connected to a Model SSC5200H Disk Station. Thermograms (sample size 0.003–0.010 g) were recorded at the scanning rate of 2.0 °C min^{-1}.

NMR spectroscopy

Solution NMR spectra were recorded on a Bruker DRX 400 (9.4 T, 400.13 MHz for ^1H, 100.62 MHz for ^{13}C and 40.56 MHz for ^{15}N) spectrometer with a 5-mm inverse-detection H—X probe equipped with a z-gradient coil, at 300 K.[30] Chemical shifts (δ in ppm) are given from internal solvent, $CDCl_3$ 7.26 for ^1H and 77.0 for ^{13}C, DMSO-d_6 2.49 for ^1H and 39.5 for ^{13}C, THF-d_8 3.58 for ^1H and 67.6 for ^{13}C, CD_3CN 1.94 for ^1H and 118.7 for ^{13}C and for ^{15}N-NMR nitromethane (0.0) was used as external standard. The spectra done in TFA solution was recorded with a lock capillary with DMSO-d_6 2.49 for ^1H and 39.5 for ^{13}C. Typical parameters for ^1H-NMR spectra were spectral width 7000 Hz and pulse width 7.5 μs at an attenuation level of 0 dB and resolution 0.15–0.25 Hz per point. Typical parameters for ^{13}C-NMR spectra were spectral width 21 kHz, pulse width 10.6 μs at an attenuation level of −6 dB, resolution 0.6 Hz per point and relaxation delay 2 s; WALTZ-16 was used for broadband proton decoupling; the FIDS were multiplied by an exponential weighting (lb = 2 Hz) before Fourier transformation. 2D inverse proton detected heteronuclear shift correlation spectra, (^1H–^{13}C) gs-HMQC, (^1H–^{13}C) gs-HMBC and (^1H–^{15}N) gs-HMBC, were acquired and processed using standard Bruker NMR software and in non-phase-sensitive mode. Gradient selection was achieved through a 5% sine truncated shaped pulse gradient of 1 ms. Selected parameters for (^1H–^{13}C) gs-HMQC and gs-HMBC spectra were spectral width 2500–8000 Hz for ^1H and 12.0 kHz for ^{13}C, 1024 × 256 data set, number of scans 2 (gs-HMQC) or 4 (gs-HMBC) and relaxation delay 1 s. The FIDs were processed using zero filling in the *F*1 domain and a sine-bell window function in both dimensions was applied prior to Fourier transformation. In the gs-HMQC experiments GARP modulation of ^{13}C was used for decoupling. Selected parameters for (^1H-^{15}N) gs-HMBC spectra were spectral width 2500–3500 Hz for ^1H and 12.5 kHz for ^{15}N, 1024 × 512 data set, number of scans 4–16, relaxation delay 1 s, 37–150 ms delay for the evolution of the ^{15}N- ^1H long-range coupling. The FIDs were processed using zero filling in the *F*1 domain and a sine-bell window function in both dimensions was applied prior to Fourier transformation.

Solid state ^{13}C (100.73 MHz) and ^{15}N (40.60 MHz) CPMAS NMR spectra have been obtained on a Bruker WB 400 spectrometer at 300 K using a 4 mm DVT probehead. Samples were carefully packed in a 4-mm diameter cylindrical zirconia rotor with Kel-F end-caps. Operating conditions involved 3.2 μs 90 ^1H pulses and decoupling

DOI: 10.1002/poc

field strength of 78.1 kHz by TPPM sequence. ^{13}C spectra were originally referenced to a glycine sample and then the chemical shifts were recalculated to the Me_4Si [for the carbonyl atom δ (glycine) = 176.1 ppm] and ^{15}N spectra to $^{15}NH_4Cl$ and then converted to nitromethane scale using the relationship: $\delta^{15}N(MeNO_2) = \delta\ ^{15}N(NH_4Cl) - 338.1$ ppm. Typical acquisition parameters for ^{13}C CPMAS were: spectral width, 40 kHz; recycle delay, 5–30 s; acquisition time, 30 ms; contact time, 2–4 ms; and spin rate, 12 kHz. In order to distinguish protonated and unprotonated carbon atoms, the Non-Quaternary Suppression (NQS) experiment by conventional cross-polarization was recorded; before the acquisition the decoupler is switched off for a very short time of 25 μs.[31,32] Typical acquisition parameters for ^{15}N CPMAS were: spectral width, 40 kHz; recycle delay, 5–30 s; acquisition time, 35 ms; contact time, 4 ms; and spin rate, 6 kHz.

DFT calculations

The optimisation of the structures of all compounds discussed in this paper was carried out at the hybrid B3LYP/6-31G** level[25,26] with basis sets of Gaussian type functions using Spartan '02 for Windows.[33]

Electronic spectra

UV–Visible spectra were measured on Shimadzu UV-250rPC UV–Visible spectrometer.

Syntheses

Compounds (**8**–**13**) have been prepared by refluxing in toluene equimolar amounts of 3-hydroxypyridine-4-carboxaldehyde (**1**) and the corresponding anilines (**2**–**7**) in toluene with quantitative yields.[6]

(*E*)-4-[(4-methoxyphenylimino)methyl]-3-hydroxypyridinium tetrafluoroborate ($10H^+BF_4^-$). Equimolar amounts of imine **10** (158 mg, 0.69 mmol) and tetrafluoroboric acid 54 wt% solution in diethyl ether (112.69 mg, 0.69 mmol) were mixed in $CHCl_3$ (25 ml) and stirred with a magnetic bar at room temperature. Immediately a red solid precipitates in the media. After filtration, the solid was washed twice with $CHCl_3$ to remove possible rests of starting materials. The crystals were purified by crystallisation (THF/$CHCl_3$); mp 181.9 °C, and 189.2 °C (DSC) with a lost at 153.9 °C.

^{1}H-NMR (DMSO-d_6), δ: 3.82 (s, 3H, OCH_3), 7.08 (m, 2H, H3′/H5′), 7.57 (m, 2H, H2′/H6′), 8.08 (d, 1H, $J = 5.6$ Hz, H5), 8.40 (d, 1H, $J = 5.6$ Hz, H6), 8.59 (s, 1H, H2) and 9.12 (s, 1H, CH═N).

^{13}C-NMR (DMSO-d_6), δ: 55.6 (OCH_3, $^1J = 145.0$ Hz), 114.9 (C3′/C5′, $^1J = 161.4$ Hz, $^3J = 4.8$ Hz), 123.8 (C2′/C6′, $^1J = 160.9$ Hz, $^3J = 6.2$ Hz), 125.9 (C5, $^1J = 171.7$, $^3J = 6.0$, $^2J = 2.4$), 132.0 (C4), 133.2 (C2, $^1J = 188.6$, $^3J = 8.1$), 133.5 (C6, $^1J = 191.3$, $^3J = 7.2$, $^2J = 4.2$), 139.8 (C1′, $^3J = {}^3J = {}^3J = 8.7$ Hz) 155.2, (CH═N, $^1J = 172.3$, $^3J = 5.3$), 156.3 (C3, $^3J = 4.6$, $^3J = 7.1$) and 160.2 (C4′).

^{1}H-NMR (THF-d_8), we observed two species **a**, 66%, **b**, 34%. **a**, δ: 3.85 (s, 3H, OCH_3), 7.05 (m, 2H, H3′/H5′), 7.60 (m, 2H, H2′/H6′), 8.11 (d, 1H, $J = 5.8$ Hz, H5), 8.47 (d, 1H, $J = 5.8$ Hz, H6), 8.57 (s, 1H, H2) and 9.14 (s, 1H, CH═N); **b**, δ: 3.80 (s, 3H, OCH_3), 7.05 (m, 2H, H3′/H5′), 7.57 (m, 2H, H2′/H6′), 7.92 (d, 1H, $J = 5.9$ Hz, H5), 8.30 (d, 1H, $J = 5.9$ Hz, H6), 8.43 (s, 1H, H2) and 9.05 (s, 1H, CH═N).

^{13}C-NMR (THF-d_8) **a**, δ: 56.1 (OCH_3), 115.9 (C3′/C5′), 125.0 (C2′/C6′), 128.7 (C5), 133.6 (C2), 134.1 (C6), 135.0 (C4), 140.3 (C1′), 157.5 (CH═N), 158.8 (C3) and 162.4 (C4′); **b**, δ: 56.0 (OCH_3), 116.0 (C3′/C5′), 124.6 (C2′/C6′), 127.7 (C5), 135.0 (C2), 134.8 (C6), 134.9 (C4), 140.5 (C1′), 157.6 (CH═N, C3) and 161.1 (C4′).

^{1}H-NMR (CD_3OD), we observed two species: **$10H^+BF_4^-$**, δ: 3.88 (s, 3H, OCH_3), 7.08 (m, 2H, H3′/H5′), 7.60 (m, 2H, H2′/H6′), 8.15 (d, 1H, $J = 5.8$ Hz, H5), 8.37 (d, 1H, $J = 5.8$ Hz, H6), 8.55 (s, 1H, H2) and 9.12 (s, 1H, CH═N); and the *addition product*, δ: 3.83 (s, 3H, OCH_3), 5.90 (s, 1H, —CH—NH—), 7.06 (m, 2H, H3′/H5′), 7.31 (m, 2H, H2′/H6′), 8.07 (d, 1H, $J = 5.8$ Hz, H5), 8.34 (d, 1H, $J = 5.8$ Hz, H6) and 8.26 (s, 1H, H2).

(*E*)-4-[(4-bromophenylimino)methyl]-3-hydroxypyridinium tetrafluoroborate ($11H^+BF_4^-$). Equimolar amounts of imine **11** (116 mg, 0.42 mmol) and tetrafluoroboric acid 54 wt% solution in diethyl ether (68.6 mg, 0.42 mmol) were mixed in $CHCl_3$ (25 ml) and stirred with a magnetic bar at room temperature. Instantly a strong orange solid precipitates in the media solution. After filtration, the solid was washed twice with $CHCl_3$ to remove possible rests of starting materials. The crystals were purified by crystallisation (THF/$CHCl_3$); mp 216.1 °C with a lost at 139.1 °C, and 227.7 decomposes (DSC).

^{1}H-NMR (THF-d_8), we observed two species **a**, 70%, **b**, 30%. **a**, δ: 7.53 (m, 2H, H3′/H5′), 7.55 (m, 2H, H2′/H6′), 8.31 (d, 1H, $J = 5.8$ Hz, H5), 8.53 (d, 1H, $J = 5.8$ Hz, H6), 8.66 (s, 1H, H2) and 9.23 (s, 1H, CH═N); **b**, δ: 7.49 (m, 2H, H3′/H5′), 7.54 (m, 2H, H2′/H6′), 8.01 (d, 1H, $J = 5.8$ Hz, H5), 8.33 (d, 1H, $J = 5.8$ Hz, H6), 8.47 (s, 1H, H2) and 9.10 (s, 1H, CH═N).

^{13}C-NMR (THF-d_8) **a/b**, δ: 123.7 (C4), 125.0 (C2′/C6′), 128.2 (C5), 133.9 (C3′/C5′), 135.5/135.2 (C2), 135.8 (C6), 158.4 (C3), 147.4 (C1′) and 162.8/161.5 (CH═N); CP-MAS δ: 119.2 (C2′/C6′), 130.0 (C4), 130.6 (C3′/C5′, C5), 132.0 (C4′), 133.4 (C6, C2), 143.1 (C1′) 157.7 (CH═N) and 158.6 (C3).

Complex (*E*)-4-[(4-bromophenylimino)methyl]-3-hydroxypyridine picric acid (11·Picric acid). Equimolar amounts of imine **11** (20 mg, 0.07 mmol) and picric acid (16.6 mg, 0.07 mmol) were mixed in $CHCl_3$ at room temperature. The solution was extracted three times with water, and the solvent was evaporated under reduce pressure giving a yellow solid of **11·Picric acid** (quantitative yield).

DOI: 10.1002/poc

^{1}H-NMR (DMSO-d_6), δ: 7.44 (m, 2H, H3′/H5′), 7.69 (m, 2H, H2′/H6′), 8.04 (d, 1H, $J = 5.4$ Hz, H5), 8.37 (d, 1H, $J = 5.4$ Hz, H6), 8.54 (s, 1H, H2), 8.58 (s, 2H, H3″/H5″) and 9.04 (s, 1H, CH═N).

^{13}C-NMR (DMSO-d_6), δ: 121.2 (C4′), 123.9 (C2′/C6′, $^1J = 162.4$ Hz, $^3J = 5.9$ Hz), 124.3 (C4), 125.2 (C5 and C3″/C5″, $^1J = 167.6$ Hz, $^3J = 5.8$ Hz), 132.4 (C3′/C5′, $^1J = 167.3$ Hz, $^3J = 5.6$ Hz), 134.4 (C6, $^1J = 186.5$ Hz), 134.7 (C2, $^1J = 186.5$ Hz), 141.8 (C2″/C6″), 147.4 (C1′ and C4″), 155.7 (C3), 158.0 (CH═N, $^1J = 171.6$ Hz) and 160.8 (C1″).

X-Ray data collection and structure refinement. Light-yellow needles single crystals of (**11H$^+$BF$_4^-$**) suitable for X-ray diffraction experiments were obtained by crystallization from THF/$CHCl_3$. Data collection were carried out at room temperature on a Bruker Smart CCD diffractometer using graphite-monochromated Mo-Kα radiation ($\lambda = 0.71073$ Å) operating at 50 kV and 30 mA. The data were collected over a hemisphere of the reciprocal space by combination of three exposure sets. Each exposure of 30 s covered 0.3 in ω. The first 100 frames were recollected at the end of the data collection to monitor crystal decay. No appreciable drop in the intensities of standard reflections was observed. The cell parameters were determined and refined by a least-squares fit of all reflections.

A summary of the fundamental crystal and refinement data of **11H$^+$BF4$^-$** is given in Table 12. The structure was solved by direct methods and conventional Fourier techniques. The refinement was done by full-matrix least-squares on F^2 (SHELXS-97).[34] In the last cycles of refinement a residual electronic density was assigned to a disordered water molecule in two positions with 0.5/0.5 occupancy. Anisotropic parameters were used in the last cycles of refinement for all non-hydrogen atoms with some exceptions. The fluorine atoms of the BF_4 anion are disordered over two positions which were refined isotropically with an occupancy of 0.5/0.5. Hydrogen atoms bonded to N1 and O1 atoms have been located in a Fourier synthesis, included and refined as riding on their respective bonded atoms. The hydrogen atoms for the water molecule were not observed in the difference maps and were not included in the model. The remaining hydrogen atoms were included in calculated positions and refined as riding on their respective carbon atoms. Largest peaks and holes in the final difference map were 0.763 and −1.170 eÅ^{-3}. Final $R(Rw)$ values were 0.0666 (0.2204). These values can be somewhat high since the crystal diffracted poorly partly due to its needle shape that gave rise to a low ratio: observed/unique reflections.

CCDC-637109 contains the supplementary crystallographic data for this paper. These data can be obtained free charge via www.ccdc.cam.ac.uk/conts/retrieving.html (or from the Cambridge Crystallographic Data Centre, 12 Union Road, Cambridge CB2 1EZ, UK; fax: (+44) 1223-336033; or www.deposit@ccde.cam.uk).

Table 12. Crystal and refinement data for 2-(*E*)-4-[(4-bromophenylimino)methyl]-3-hydroxypyridinium tetrafluoroborate (**11H$^+$BF$_4^-$**)

CCDC number	637109
Empirical formula	$C_{12}H_{10}$ $BrN_2O.BF_4O$
Formula weight	380.94
Crystal system	Monoclinic
Space group	$P2_1/c$
a (Å)	9.278(1)
b (Å)	7.345(1)
c (Å)	22.346(3)
β (°)	97.632(2)
V (Å^3)	1509.3(3)
Z	4
T (K)	296(2)
F(000)	752
$\rho_{calc.}$ (g cm^{-3})	1.685
μ (mm^{-1})	2.773
Scan technique	ω and φ
Data collected	(−9,−8,−26) to (11,8,26)
θ range (°)	1.84–25
Reflections collected	11156
Independent reflections	2656 ($R_{int} = 0.1296$)
Completeness to maximum θ	100%
Data/restraints/parameters	2656/0/206
GOF (F^2)	1.025
R $[I > 2\sigma(I)]$[a]	0.0666 (1271 observed refl.)
RW_F (all data)[b]	0.2204
Largest residual peak (e Å^{-3})	0.742 and −0.644

[a] $\Sigma[|F_o|-|F_c|]/\Sigma|F_o|$.
[b] $\{\Sigma[w(F_o^2-F_c^2)^2]/\Sigma[w(F_o^2)^2]\}^{1/2}$.

Acknowledgements

This work was supported by DGES/MEyC (BQU2003-00976 and CTQ2006-02586) of Spain. One of us (A.P.) is indebted to the MCyT of Spain for an FPI grant.

REFERENCES

1. Kohan A, Klinman JP. *Acc. Chem. Res.* 1998; **31**: 397–404.
2. Ingham KC, El-Bayoumi MA. *J. Am. Chem. Soc.* 1974; **96**: 1674–1682.
3. That QT, Nguyen KPP, Hansen PE. *Magn. Reson. Chem.* 2005; **43**: 302–308.
4. Rozwadowski Z, Majewski E, Dziembowska T, Hansen PE. *J. Chem. Soc. Perkin Trans. 2.* 1999; 2809–2819.
5. Hansen PE, Sitkowwski J, Stefaniak L, Rozwadowski Z, Dziembowska T. *Ber. Bunsen. Phys. Chem.* 1998; **102**: 410–413.
6. Sanz D, Perona A, Claramunt RM, Elguero J. *Tetrahedron* 2005; **61**: 145–154.
7. Roussel R, Oteyza de Guerrero M, Spegt P, Galin JC. *J. Heterocycl. Chem.* 1982; **19**: 785–796.
8. (a) Kolehmainen E, Ośmiabwski B, Krygowski TM, Kauppinen R, Nissinen M, Gawinecki R. *J. Chem. Soc. Perkin Trans. 2* 2000; 1259–1266; (b) Kolehmainen E, Ośmiabwski B, Krygowski TM, Kauppinen R, Nissinen M, Gawinecki R. *J. Chem. Soc. Perkin Trans. 2* 2000; 2185–2191.
9. Kabachnik MI, Mastrukova TA, Shipov AE, Melentyeva TA. *Tetrahedron* 1960; **9**: 10–28.

DOI: 10.1002/poc

10. Iglesias E, Ojea-Cao V, García-Rio L, Leis JR. *J. Org. Chem.* 1999; **64**: 3954–3963.
11. Christen P, Metzler DE. *Transaminases*. Wiley: New York, 1985.
12. (a) Claramunt RM, Sanz D, Boyer G, Catalán J, de Paz JL, Elguero J. *Magn. Reson. Chem.* 1993; **31**: 791–800; (b) Claramunt RM, Sanz D, Catalán J, Fabero F, García NA, Foces-Foces C, Llamas-Saiz AL, Elguero J. *J. Chem. Soc. Perkin Trans. 2* 1993; 1687–1699.
13. Alarcón SH, Olivieri AC, Sanz D, Claramunt RM, Elguero J. *J. Mol. Struct.* 2004; **705**: 1–9.
14. Martin GJ, Martin ML, Gouesnard JP. *^{15}N-NMR Spectroscopy*. Springer-Verlag: Berlin, 1981.
15. (a) Perona A, Sanz D, Claramunt RM, Elguero J. *Molecules* 2006; 453–463.; (b) Sanz D, Perona A, Claramunt RM, Pinilla E, Torres MR, Elguero J. *Helv. Chim. Acta* 2006; **89**: 1290–1303.; (c) Claramunt RM, López C, Santa María MD, Sanz D, Elguero J. *Prog. NMR Spectrosc.* 2006; **49**: 169–206.
16. (a) Alarcon SH, Olivieri AC, Nordon A, Harris RK. *J. Chem. Soc. Perkin Trans. 2* 1996; 2293–2296; (b) Takeda S, Inabe T, Benedict C, Langer U, Limbach HH. *Ber. Bunsenges. Phys. Chem.* 1998; **102**: 1358–1369; (c) Dziembowska T, Ambroziak K, Rozwadowski Z, Schilf W, Kamieński B. *Magn. Reson. Chem.* 2003; **41**: 135–138.
17. Kamieński B, Schilf W, Rozwadowski Z, Dziembowska T, Szady-Chelmieniecka A. *Solid State NMR* 2000; **16**: 285–289.
18. Foces-Foces C, Echevarria A, Jagerovic N, Alkorta I, Elguero J, Langer U, Klein O, Minguet-Bonvehi M, Limbach HH. *J. Am. Chem. Soc.* 2001; **123**: 7898–7906.
19. Witanowski M, Stefaniak L, Webb G. *Annu. Rep. NMR Spectrosc.* 1991; **11B**: 95–96.
20. Schilf W, Kamieński B, Dziembowska T. *J. Mol. Struct* 2002; **41**: 602–603.
21. Llamas-Saiz AL, Foces-Foces C, Echevarria A, Elguero J. *Acta Crystallogr., Sect. C.* 1995; **51**: 1401–1404.
22. Gawinecki R, Raczyńska ED, Rasała D, Styrcz S. *Tetrahedron* 1997; **53**: 17211–17220.
23. Valdés-Martinez J, Rubio M, Rosado RC, Salcedo-Loaiza J, Toscano RA, Espinosa-Perez G, Hernandez-Ortega S, Ebert K. *J. Chem. Crystallogr.* 1997; **27**: 627–634.
24. Janiak Ch. *Dalton Trans.* 2000; 3885–3896.
25. (a) Becke AD. *Phys. Rev. A* 1988; **38**: 3098–3100; (b) Becke AD. *J. Chem. Phys.* 1993; **98**: 5648–5652; (c) Lee C, Yang W, Parr RG. *Phys. Rev. B* 1988; **37**: 785–789; (d) Miehlich B, Savin A, Stoll H, Preuss H. *Chem. Phys. Lett.* 1989; **157**: 200–206.
26. Hariharan PC, Pople JA. *Theor. Chim. Acta* 1973; **28**: 213–222.
27. Frey PA. *Magn. Reson. Chem.* 2001; **39**: S190–S198.
28. Schirch L, Slotter RA. *Biochemistry* 1966; **5**: 3175–3181.
29. Sharif S, Denisov GS, Toney MD, Limbach HH. *J. Am. Chem. Soc.* 2006; **128**: 3375–3387.
30. Berger S, Braun S. *200 and More NMR Experiments*. Wiley-VCH: Weinheim, 2004.
31. (a) Murphy PD. *J. Magn. Reson.* 1983; **52**: 343–345; (b) Murphy PD. *J. Magn. Reson.* 1985; **62**: 303–308.
32. Alemany LB, Grant DM, Alger TD, Pugmire RJ. *J. Am. Chem. Soc.* 1983; **105**: 6697–6704.
33. Spartan 2002 for Windows from Wavefuntion Inc.
34. Sheldrick GM. *SHELX97. Program for Refinement of Crystal Structure*. University of Göttingen: Göttingen, Germany, 1997.

DOI: 10.1002/poc